Smart Structures and Systems, *Vol. 14, No. 5 (2014) 847-867*
DOI: http://dx.doi.org/10.12989/sss.2014.14.5.847

A new methodology of the development of seismic fragility curves

Young-Joo Lee[1a] and Do-Soo Moon[*2]

[1]School of Urban and Environmental Engineering, Ulsan National Institute of Science and Technology, Ulsan 689-798, Republic of Korea
[2]Department of Civil and Environmental Engineering, University of Illinois at Urbana-Champaign, Urbana, IL 61801, USA

(Received March 4, 2013, Revised August 20, 2013, Accepted December 11, 2013)

Abstract. There are continuous efforts to mitigate structural losses from earthquakes and manage risk through seismic risk assessment; seismic fragility curves are widely accepted as an essential tool of such efforts. Seismic fragility curves can be classified into four groups based on how they are derived: empirical, judgmental, analytical, and hybrid. Analytical fragility curves are the most widely used and can be further categorized into two subgroups, depending on whether an analytical function or simulation method is used. Although both methods have shown decent performances for many seismic fragility problems, they often oversimplify the given problems in reliability or structural analyses owing to their built-in assumptions. In this paper, a new method is proposed for the development of seismic fragility curves. Integration with sophisticated software packages for reliability analysis (FERUM) and structural analysis (ZEUS-NL) allows the new method to obtain more accurate seismic fragility curves for less computational cost. Because the proposed method performs reliability analysis using the first-order reliability method, it provides component probabilities as well as useful byproducts and allows further fragility analysis at the system level. The new method was applied to a numerical example of a 2D frame structure, and the results were compared with those by Monte Carlo simulation. The method was found to generate seismic fragility curves more accurately and efficiently. Also, the effect of system reliability analysis on the development of seismic fragility curves was investigated using the given numerical example and its necessity was discussed.

Keywords: seismic fragility curve; seismic risk assessment; earthquake loss; reliability analysis; system reliability; first order reliability method; Monte Carlo simulation

1. Introduction

The losses caused by earthquakes in the past few decades have been dramatically increasing worldwide (Calvi *et al*. 2006, DesRoches *et al*. 2011). Accordingly, there have been continuous efforts to estimate earthquake losses and manage the risk through seismic risk assessment in various ways, such as structural maintenance, structural management, disaster mitigation, and emergency response. Seismic fragility curves are widely accepted as an indispensable tool to these

∗Corresponding author, Postdoctoral Research Associate, E-mail: dmoon3@illinois.edu
[a] Assistant Professor, E-mail: ylee@unist.ac.kr

http://www.techno-press.org/?journal=sss&subpage=8 ISSN: 1738-1584 (Print), 1738-1991 (Online)

efforts. For example, software packages for seismic risk assessment such as HAZUS (NIBS 1999) and MAEviz (Elnashai *et al*. 2008) employ seismic fragility curves and evaluate a variety of post-earthquake losses under certain earthquake scenarios based on these curves. Such estimates provide the user with a basis for decision-making concerning structural inspection, repair, and management and for strategizing to reduce losses (Kircher *et al*. 2006). Thus, the development of accurate seismic fragility curves is a key to effective seismic risk assessment and management.

A seismic fragility curve is defined as the relationship between the ground-shaking intensity (e.g., peak ground acceleration (PGA) or spectral acceleration) and the probability that a structure reaches or exceeds a certain response level (Jeong and Elnashai 2007). There are several ways to derive seismic fragility curves. Existing fragility curves can be categorized into four groups (Rossetto and Elnashai 2003) depending on how the damage data are obtained: empirical (from post-earthquake surveys), judgmental (from expert opinion), analytical (from analytical approaches), and hybrid (from combinations of the prior three). Although empirical and judgmental fragility curves may be more realistic because they are derived from actual structures, they are limited in general applications (Kwon 2007).

Thus, analytical methods are widely used for the development of seismic fragility curves; they can be further categorized depending on whether an analytical function or simulation is used (Rossetto and Elnashai 2003). In analytical-function–based methods, the seismic fragility of a structure is explicitly expressed as an analytical function of related parameters such as the PGA or PGV (peak ground velocity), natural period of the structure, and response threshold of interest. However, the estimates from the structural analysis are commonly oversimplified for the sake of the derivation. In most cases, only single-degree-of-freedom analysis or static analysis is allowed rather than inelastic dynamic response-history analysis owing to the assumptions of this approach (Kwon 2007). Considering that reliability and structural analyses are the two cores of seismic fragility analysis, analytical-function–based methods allow rigorous performance of the former but not the latter.

In simulation-based methods, seismic fragility curves can be obtained through more rigorous structural analysis. These methods generally require generating a certain number of random variable sets, performing structural analysis for each one, and checking if the corresponding structural response exceeds a threshold or not. With the simulation-based approach, structural analysis is done rigorously because sophisticated structural analysis (e.g., inelastic pushover analysis or inelastic dynamic response-history analysis) can be introduced. Also, simulation methods (e.g., Monte Carlo simulation (MCS)) have obtained a good reputation for accuracy with regard to reliability analysis. However, simulation-based methods often require a huge number of structural analyses for reliable outcomes, and the efficiency of the fragility analysis may suffer when sophisticated and expensive structural analysis needs to be introduced.

To overcome the disadvantages of existing analytical methods for seismic fragility curve development, this paper introduces a new analytical method. In the proposed method, the fragility estimate is neither explicitly expressed by a function of related parameters or evaluated using simulation techniques. Instead, two sophisticated reliability analysis and structural analysis packages are coupled in order to get more accurate seismic fragility curves. The reliability analysis package utilizes the non-simulation-based technique (FORM) for better computational efficiency. To the best of the author's knowledge, there is no method employing such a coupling technique for the development of seismic fragility curves. The proposed method can be categorized as a new analytical method.

2. Reliability analysis methods

A number of reliability analysis methods have been developed and adopted in various engineering disciplines (Haldar 2006). They can be classified into two groups: simulation-based and analytical (or non-simulation-based) methods. Representative types include MCS and the first-order reliability method (FORM), respectively. Melchers (1999) and Der Kiureghian (2005) provide detailed reviews of the two methods. In this study, FORM was used to overcome the disadvantages of using MCS to derive seismic fragility curves. The methods are briefly introduced here for comparison purposes.

2.1 First-order reliability method (FORM)

Consider a limit-state function that expresses an event of interest. In a structural reliability problem, the limit-state function is termed $g(\mathbf{x})$, and the event of interest (often called "failure") is expressed by $g(\mathbf{x}) \leq 0$, where $\mathbf{x}$ is a column vector of n random variables (i.e., $\mathbf{x} = [x_1, x_2, \ldots, x_n]^T$) representing the uncertainties in the given problem. Then, the probability of the event P_f is

$$P_f = P[g(\mathbf{x}) \leq 0] = \int_{g(\mathbf{x}) \leq 0} f_{\mathbf{x}}(\mathbf{x}) d\mathbf{x} \tag{1}$$

where $f_{\mathbf{x}}(\mathbf{x})$ is the joint probability density function (PDF) of $\mathbf{x}$. By transforming the space of random variables into the standard normal space, the probability P_f can be expressed as

$$P_f = \int_{g(\mathbf{x}) \leq 0} f_{\mathbf{x}}(\mathbf{x}) d\mathbf{x} = \int_{G(\mathbf{u}) \leq 0} \varphi_n(\mathbf{u}) d\mathbf{u} \tag{2}$$

where $G(\mathbf{u}) = g(\mathbf{T}^{-1}(\mathbf{u}))$ is the transformed limit-state function in the standard normal space, $\varphi_n(\cdot)$ denotes the n-th order standard normal PDF, $\mathbf{u}$ is the column vector of n standard normal variables, and $\mathbf{T}$ is the one-to-one mapping transformation matrix that satisfies $\mathbf{u} = \mathbf{T}(\mathbf{x})$.

In FORM, the probability (i.e., P_f in Eq. (2)) can be approximated by linearizing the function $G(\mathbf{u})$ at the point $\mathbf{u}^*$ that is defined by the following constrained optimization problem

$$\mathbf{u}^* = \arg\min \left\{ \|\mathbf{u}\| \,|\, G(\mathbf{u}) = 0 \right\} \tag{3}$$

where "arg min" denotes the argument of the minimum of a function and $\|\cdot\|$ is the L^2-norm. In Eq. (3), $\mathbf{u}^*$ is located on the limit-state surface satisfying $G(\mathbf{u}) = 0$ and has the minimum distance from the origin in the standard normal space. As an example of the first-order approximation concept of the FORM, Fig. 1 shows the approximated limit-state function in the two-dimensional space.

In the standard normal space shown in the figure, because equal probability density contours are concentric circles centered at the origin, $\mathbf{u}^*$ has the highest probability among all of the nodes in the failure domain $G(\mathbf{u}) \leq 0$. In this sense, $\mathbf{u}^*$ is an optimal point and is commonly called the *design point* or *most probable point* (MPP).

Noting that $G(\mathbf{u}^*) = 0$, the limit-state function approximated at MPP is written as

$$G(\mathbf{u}) \cong \nabla G(\mathbf{u}^*)(\mathbf{u} - \mathbf{u}^*) = \|\nabla G(\mathbf{u}^*)\|(\beta - \alpha\mathbf{u}) \tag{4}$$

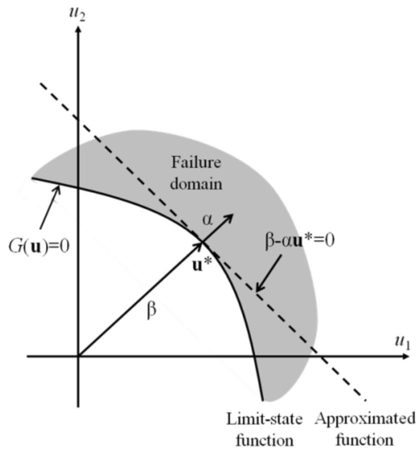

Fig. 1 Linear approximation in FORM

where $\nabla G(\mathbf{u}) = [\partial G/\partial u_1,\ldots, \partial G/\partial u_n]$ denotes the gradient vector, $\boldsymbol{\alpha} = -\nabla G(\mathbf{u^*})/\|\nabla G(\mathbf{u^*})\|$ is the normalized negative gradient vector at MPP (i.e., a unit vector normal to the limit-state surface at MPP), and $\beta = -\boldsymbol{\alpha}\mathbf{u}^*$ is the reliability index.

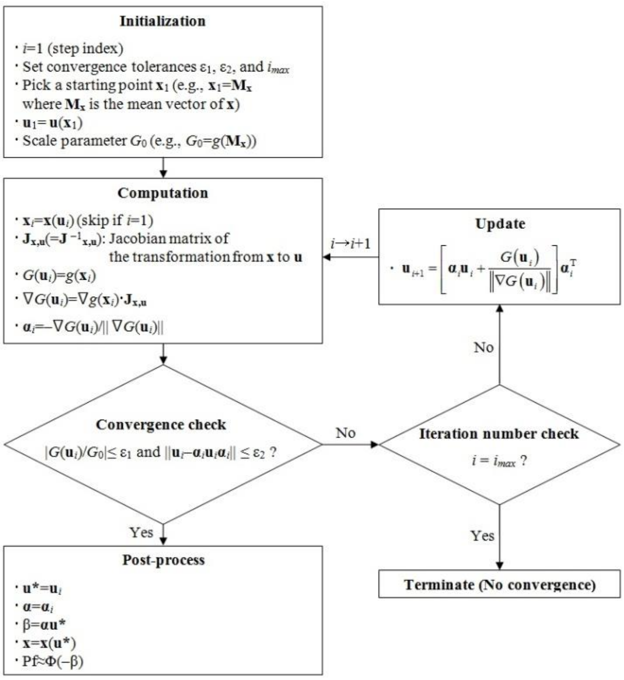

Fig. 2 FORM by HL-RF algorithm (Song 2007)

A representative method for solving the constrained optimization problem in Eq. (3) is the HL-RF algorithm, which is summarized in Fig. 2. Rackwitz and Fiessler (1978) and Der Kiureghian (2005) provide details on the algorithm and FORM. In the following numerical example, ε_1, ε_2, and i_{max} were assumed to be 0.05, 0.05, and 20, respectively.

2.2 Monte Carlo simulation (MCS)

Compared with FORM, MCS is conceptually straightforward. To estimate the failure probability in a structural reliability problem, n_s sample sets of random variables need to be generated. Each random variable set is used to run a structural analysis and check whether the given structure fails or not. The failure probability P_f is

$$P_f = n_f / n_s \tag{5}$$

where n_f is the number of sample sets that satisfy $g(\mathbf{x}) \leq 0$. Unlike FORM, the result from MCS is not a closed-form solution and always has a sampling error. The MCS result converges to a closed-form solution as the number of samples increases, but the error cannot be completely eliminated unless the number of samples is infinite.

Furthermore, MCS can be very expensive computationally, and the convergence of the failure probability result may be slow depending on the structural analysis cost. According to Haldar and Mahadevan (2000), the minimum number of samples (N_δ) to achieve a target coefficient of variation (δ) is calculated by

$$N_\delta = \frac{1-P_f}{\delta^2 P_f} \tag{6}$$

where P_f is the failure probability from MCS.

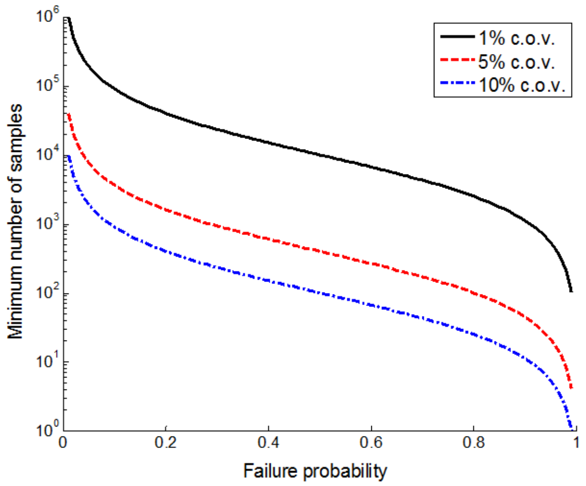

Fig. 3 Minimum number of samples with varying failure probability and coefficient of variation

Fig. 3 shows the relationship between the minimum number of samples (N_δ) and failure probability (P_f) for several coefficients of variation (δ) in semi-log scale. To achieve a 5% coefficient of variation, which is often accepted by researchers as reasonable, for expected failure probabilities of 0.1, 0.05, and 0.01, then 3.6×10^3, 7.6×10^3, and 3.96×10^4 samples need to be used along with the same numbers of structural analyses. Furthermore, the computational cost significantly increases if a lower level of probability or high level of convergence (i.e., low coefficient of variation value) is expected for the failure probability calculation. However, performing such a huge number of structural analyses is impractical, even if each analysis takes only a few minutes. When each structural analysis is expensive (such as nonlinear inelastic response history analysis), achieving a reliable level of failure probability using MCS is almost impossible.

3. Seismic fragility analysis platform integrated with FERUM and ZEUS-NL

To overcome the shortcomings of MCS and introduce FORM into fragility curve development, two software packages for reliability and structural analyses were coupled. According to Haukaas (2003), Der Kiureghian and Taylor (1983) were the first to attempt to couple reliability analysis algorithms and structural analysis methods. Since then, many studies have developed various software packages for structural reliability analysis. These developed software packages can be categorized into two groups depending on how the structural analysis module is integrated with the reliability analysis module. Programs of the first group such as CalREL (Liu *et al*. 1989) and FERUM (Haukaas *et al*. 2003) express the probabilistic model by algebraic functions or user-defined algorithms involving basic random variables. These software packages have their own structural analysis modules or require users to analytically express the limit state of their interests in terms of random variables. However, most of programs in this group are limited to linear structural models.

Programs of the second group such as NESSUS (SwRI 2009) and STRUREL (Gollwitzer *et al*. 2006) allows their users to introduce sophisticated structural analysis methods to represent the structural behavior accurately. An interface code between FERUM and ABAQUS® (i.e., FERUM-ABAQUS) was developed as an extension of this trend. By coupling two software packages with different specializations, their individual advantages can be fully utilized to solve challenging structural reliability problems such as the aircraft wing torque box (Lee *et al*. 2008) and cable-stayed bridge pylon (Kang *et al*. 2012).

However, such coupling techniques have not been applied to the development of seismic fragility curves. In order to perform seismic fragility analysis based on the proposed method, two external software packages that execute reliability and structural analyses need to be coupled. In this study, FERUM and ZEUS-NL were selected; an interface code was developed so that these two software packages can communicate with each other during fragility analysis. The computational platform integrating FERUM and ZEUS-NL was termed FERUM-ZEUS. By coupling reliability analysis software (FERUM) and structural analysis software (ZEUS-NL), the new method allows more accurate seismic fragility curves to be obtained for less computational cost.

3.1 Component reliability analysis using FERUM-ZEUS

Finite Element Reliability Using Matlab (FERUM) is a reliability analysis package developed by researchers at the University of California at Berkeley and can perform various reliability analyses (Haukaas *et al*. 2003). FERUM offers functions from various reliability analysis methods including FORM, second-order reliability method, MCS, and importance sampling simulation; most of the common probability distribution types are available in the program. In addition, the programmers have made the source codes open to the public (www.ce.berkeley.edu/FERUM). Because of these attractive features, FERUM has been widely applied to various engineering problems.

ZEUS-NL (Elnashai *et al*. 2010) is a fiber-element-based nonlinear analysis program developed by the Mid-America Earthquake (MAE) Center. It is an advanced structure analysis package specifically for earthquake engineering applications. ZEUS-NL can represent the spread of inelasticity within the member cross-section as well as along the member length by utilizing the fiber analysis approach. Its source code is also open to the public (http://code.google.com/p/zeus-nl/).

Fig. 4 shows the data flow in FERUM-ZEUS. As a numerical example, we used the FORM available from the open-source FERUM. In order to solve the nonlinear constrained optimization problem in Eq. (3) using FORM, as shown in Fig. 2, $G(\mathbf{u}_i)$ and $\nabla G(\mathbf{u}_i)$ (i.e., values and gradients of the limit-state function in the standard normal space) are required at each step of the iteration. If the limit-state function is expressed by random variables $\mathbf{x}$, the gradient values can also be obtained analytically (i.e., by $\nabla G(\mathbf{u}_i) = \nabla g(\mathbf{u}_i)\cdot\mathbf{J}_{\mathbf{x},\mathbf{u}}$). However, if the limit-state function is not an analytical function of a random variable, calculating the gradients during the FORM is a challenging task. The interface module between FERUM and ZEUS-NL was developed so that FERUM can obtain the limit-state function values from the output responses—e.g., force or displacement results evaluated from structural analysis using ZEUS-NL—and the gradients are obtained numerically by the finite difference method. The number of limit-state function evaluations n_{fe} during FORM is

$$n_{fe} = (n_{RV} + 1) \times n_i \tag{7}$$

where n_{RV} and n_i denote the number of random variables (RVs) and number of iterations, respectively.

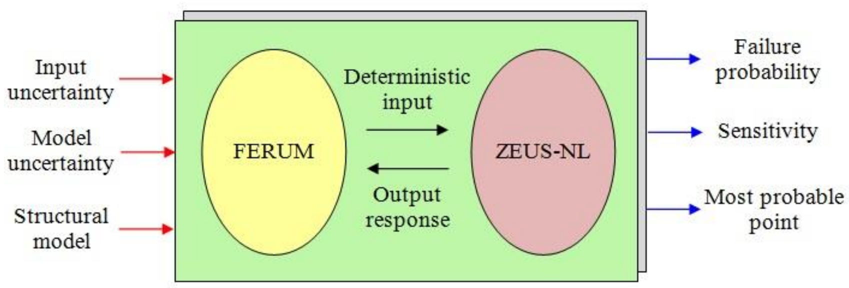

Fig. 4 Data flow in FERUM-ZEUS

In the proposed platform, the reliability analysis package FERUM repeatedly calls ZEUS-NL to obtain structural responses during the component reliability analysis with FORM. By employing ZEUS-NL, which specializes in nonlinear response history analysis, FERUM can accurately perform reliability analysis based on sophisticated structural analysis.

3.2 System reliability analysis using FERUM-ZEUS

For a complex structural system, failure may be described as a system event, which requires system reliability analysis (Song and Der Kiureghian 2003, Song and Kang 2009, Lee *et al*. 2008). In the numerical example, system reliability analysis was conducted to investigate its effect on fragility curve development.

The main goal of system reliability analysis (SRA) is to evaluate the probability of a system event that describes the failure of a structural system: that is

$$P_{sys} = P\left[\bigcup_{k}\bigcap_{i\in C_k} g_i(\mathbf{x}) \le 0\right] \tag{8}$$

where C_k denotes the index set of components in the k-th cut-set. This general “cut-set” formulation can also represent “series” systems (i.e., all of the cut-sets have only one component) and “parallel” systems (i.e., there is only one cut-set). In particular, when FORM is used for the component reliability analyses, P_{sys} can be approximated as

$$P_{sys} = P(\mathbf{\Omega}) = P\left[\bigcup_{k}\bigcap_{i\in C_k} (\beta_i - Z_i \le 0)\right] = \int_{\mathbf{\Omega}} \varphi_n(\mathbf{z};\mathbf{R})d\mathbf{z} \tag{9}$$

where Ω denotes the failure domain approximated as a polyhedron as determined by linear half spaces, $\beta_i = \boldsymbol{\alpha}_i\mathbf{u}_i^*$ is the reliability index of the i-th component event, $\mathbf{z} = \{Z_i\}$, i = 1,…, n is the vector of standard normal random variables approximately describing the component events by $\beta_i - Z_i \le 0$, $\varphi_n(\mathbf{z};\mathbf{R})$ is the joint PDF of $\mathbf{z}$, and $\mathbf{R}$ is the correlation coefficient matrix of $\mathbf{z}$ where the correlation coefficient between Z_i and Z_j is computed as $\rho_{ij} = -\boldsymbol{\alpha}_i\boldsymbol{\alpha}_j^{\mathrm{T}}$ (Hohenbichler and Rackwitz 1983). In other words, the system probability P_{sys} is computed by using the component reliability analysis results, the probabilities of component events, and their correlations

Various SRA algorithms have been developed to compute the probability of this logical function of component events from the results of individual component reliability analyses, such as theoretical bounding formulas (Ditlevsen 1979), sequentially conditioned importance sampling (Ambartzumian *et al*. 1998), the product of conditional marginals method (Pandey 1998), the multivariate normal integral method by Genz (1992) (applicable to series and parallel systems), and the first-order system reliability methods (Hohenbichler and Rackwitz 1983) (applicable to series and parallel systems directly, and to cut-set and link-set systems indirectly in conjunction with bounding formulas). However, these existing methods for system reliability analysis are applicable to “series” and “parallel” systems but not to “general” system events. In addition, they are not flexible in incorporating various types and amounts of available information on components and their statistical dependence.

Thus, SRA methods such as the linear programming bounds method (Song and Der Kiureghian 2003), matrix-based system reliability method (Song and Kang 2009), and sequential compounding method (Kang and Song 2010) have recently been developed. These methods can solve general system events and have various merits. Kang (2011) provides a more comprehensive review on SRA methods.

In the numerical example, the structural failure of interest was expressed as a series event, and the multivariate normal integral method by Genz (1992) was employed to calculate the system probability. This method specializes in series and parallel system probability calculations and has been successfully tested on various structural and non-structural reliability problems (Genz 1992, Lee and Song 2011, Lee and Song 2012).

4. Numerical example: 2D frame structure

In order to verify the proposed method and highlight its advantages, a benchmark problem was chosen and solved. Kwon and Elnashai (2006) performed fragility analyses with 2D frame structures to develop their fragility curves and investigate the effect of material and ground motion uncertainty on them. They utilized a three-story reinforced concrete frame and derived its seismic fragility curves through MCS using nine sets of input ground motions. The same structure was investigated in this study as a benchmark model. The proposed non-simulation-based method employing FERUM-ZEUS was applied to derive the fragility curves, which were compared with the MCS-derived curves of Kwon and Elnashai (2006).

4.1 Problem description

4.1.1 Analytical model

The three-story reinforced concrete moment frame used by Kwon and Elnashai (2006) was utilized as the prototype structure. As shown in Fig. 5, it had three bays in the longitudinal direction, and the length of one bay was 5.49 m (18 ft). Each story had a height of 3.66 m (12 ft), and the total height was 10.98 m (36 ft). The analytical model was created in the nonlinear finite element analysis program ZEUS-NL, as depicted in Fig. 6. Columns and beams were divided into six and seven elements, respectively. The twelve columns were labeled as C01–C04 (first story), C11–C14 (second story), and C21–C24 (third story). Lumped masses were placed at the beam–column connections. In the model, only hysteretic damping was considered with nonlinear material modeling. For detailed information, refer to Bracci *et al*. (1992) and Kwon and Elnashai (2006).

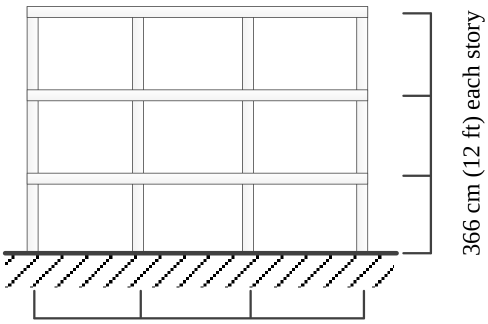

Fig. 5 Elevation view of prototype structure

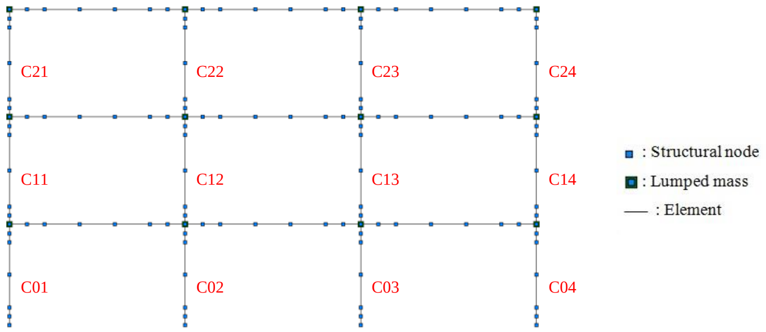

Fig. 6 Structural model constructed for FERUM-ZEUS

4.1.2 Input ground motions

Kwon and Elnashai (2006) used nine ground motion sets to derive their fragility curves. The first three sets were based on the ratio of the PGA to the PGV (*a*/*v*), and the other six were artificial ground motions generated with different soil profiles from the Memphis area. Of those nine sets, the first three ground motions sets based on the *a*/*v* ratio were employed in this study. These sets had low, intermediate, and high *a*/*v*, and each set had five input ground motions that were selected based on the following categorization.

$$\begin{aligned} &\text{Low}: a/v < 0.8g/\mathrm{m}\cdot\mathrm{s}^{-1} \\ &\text{Intermediate}: 0.8g/\mathrm{m}\cdot\mathrm{s}^{-1} \le a/v \le 1.2g/\mathrm{m}\cdot\mathrm{s}^{-1} \\ &\text{High}: 1.2g/\mathrm{m}\cdot\mathrm{s}^{-1} < a/v \end{aligned} \tag{10}$$

Table 1 summarizes the properties of the selected ground motions, and Figs. 7-9 show their acceleration time-history records.

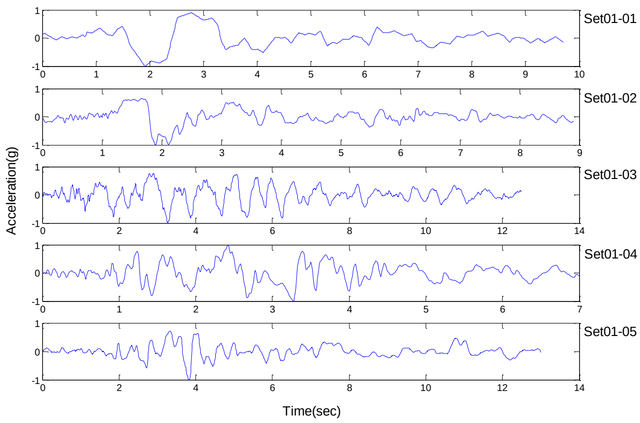

Fig. 7 Input ground motions with low *a*/v ratio

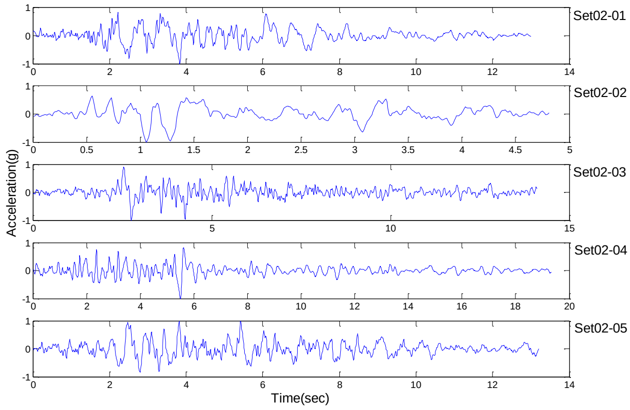

Fig. 8 Input ground motions with intermediate *a*/v ratio

Table 1 Properties of selected input ground motions, after: (Kwon and Elnashai 1980)

a/*v* ratio	Name	Earthquake event/Location	Magnitude	Date	Soil type	Distance (km)	Maximum acceleration (m/s^2)	*a*/*v* ratio (g/ms^{-1})
Low	Set01-01	Bucharest/Romania	6.40	3/4/1977	Rock	4	−1.906	0.275
	Set01-02	Erzincan/Turkey	Unknown	3/13/1992	Stiff soil	13	−3.816	0.382
	Set01-03	Aftershock of Montenegro/Yugoslavia	6.20	5/24/1979	Alluvium	8	−1.173	0.634
	Set01-04	Kalamata/Greece	5.50	9/13/1986	Stiff soil	9	−2.109	0.657
	Set01-05	Kocaeli/Turkey	Unknown	8/17/1999	Unknown	101	−3.039	0.750
Inter-mediate	Set02-01	Aftershock of Friuli/Italy	6.10	9/15/1976	Soft soil	12	−0.811	1.040
	Set02-02	Athens/Greece	Unknown	9/7/1999	Unknown	24	−1.088	1.090
	Set02-03	Umbro-Marchigiano/Italy	5.80	9/26/1997	Stiff soil	27	−0.992	1.108
	Set02-04	Lazio Abruzzo/Italy	5.70	5/7/1984	Rock	31	−0.628	1.136
	Set02-05	Basso Tirreno/Italy	5.60	4/15/1978	Soft soil	18	0.719	1.183
High	Set03-01	Gulf of Corinth/Greece	4.70	11/4/1993	Stiff soil	10	−0.673	1.432
	Set03-02	Aftershock of Montenegro/Yugoslavia	6.20	5/24/1979	Rock	32	−0.667	1.526
	Set03-03	Aftershock of Montenegro/Yugoslavia	6.20	5/24/1979	Alluvium	16	−1.709	1.564
	Set03-04	Aftershock of Umbro-Marchigiana/Italy	5.00	11/9/1997	Rock	2	0.412	1.902
	Set03-05	Friuli/Italy	6.30	5/6/1976	Rock	27	3.500	1.730

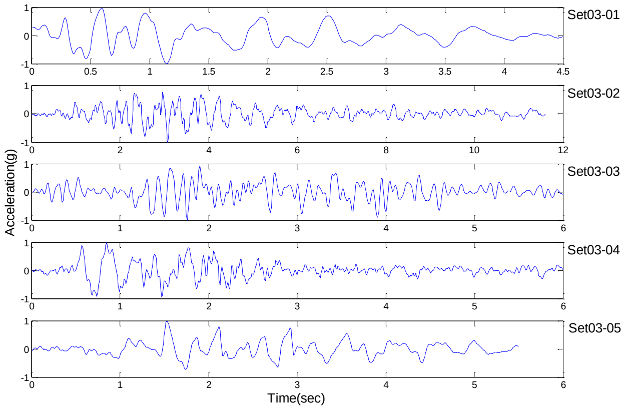

Fig. 9 Input ground motions with high *a*/v ratio

Table 2 Statistical properties of random variables

Random variables (RVs)	Mean (MPa)	Coefficient of variation	Distribution type	Number of RVs
Concrete strength (f_c)	33.6	0.186	Normal	1
Steel strength (f_y)	336.5	0.107	Normal	1

4.1.3 Statistical parameters

Three kinds of uncertainties were considered, similar to Kwon and Elnashai (2006): input ground motion, concrete strength, and steel strength. The first characterized the uncertainty in loads or demand, and the other two represented the uncertainties in the material properties or supply. Uncertainty in demand was accounted for by using sets of ground motions, whereas uncertainties in the supply were represented by two random variables: concrete and steel strength. Table 2 summarizes the mean, coefficient of variation, and type of distribution used for those random variables. The statistical properties are the same as those used by Kwon and Elnashai (2006).

4.1.4 Limit states

As defined by Kwon and Elnashai (2006), three limit states of *serviceability*, *damage control*, and *collapse prevention* were employed. The corresponding inter-story drifts are 0.57%, 1.2%, and 2.3%, respectively; they were defined from the adaptive pushover analysis of the prototype structure based on the first yielding of the steel reinforcement, maximum element strength and maximum confined concrete strain in the column members. The prototype structure had a total of twelve columns (i.e., four columns on each of three stories), and a limit state was assumed to be achieved if any column met the inter-story drift criterion. With this assumption, the limit-state functions were defined as follows

$$\text{Serviceability:}\quad g(\mathbf{x}) = 0.0057 - \max\left[ISD_{C01}(\mathbf{x}), ISD_{C02}(\mathbf{x}),..., ISD_{C24}(\mathbf{x})\right] \leq 0 \tag{11a}$$

$$\text{Damage control:}\quad g(\mathbf{x}) = 0.012 - \max\left[ISD_{C01}(\mathbf{x}), ISD_{C02}(\mathbf{x}),..., ISD_{C24}(\mathbf{x})\right] \leq 0 \tag{11b}$$

$$\text{Collapse prevention:}\quad g(\mathbf{x}) = 0.023 - \max\left[ISD_{C01}(\mathbf{x}), ISD_{C02}(\mathbf{x}),..., ISD_{C24}(\mathbf{x})\right] \leq 0 \tag{11c}$$

where ISD_{C01}, ISD_{C02},…, ISD_{C24} denote the inter-story drift (ISD) ratios of the twelve columns (C01–C04, C11–C14, and C21–C24) in Fig. 6.

4.2 Analysis results

4.2.1 Seismic fragility curves

Fig. 10 shows fragility curves from the proposed method for the three limit states. Different ground motion sets produced significant differences in the fragility curves, and the overall trend was that the exceedance probability increased with the decreasing IDS threshold and increasing PGA.

The fragility curve results from the proposed non-simulation-based method were fairly similar to those of Kwon and Elnashai (2006) using the MCS, especially at high exceedance probabilities. Some degree of discrepancy between them is clearly related to the basic difference between the two approaches. Kwon and Elnashai stated that they performed a total of 23,000 dynamic response-history analyses; that is 100 simulations (i.e., 100 structural analyses) for each input ground motion at each PGA. In order to confirm the sources of the differences and compare the computational efficiency, MCS was conducted for three selected cases, shown in Table 3, using up to 1000 samples. The proposed method calculated the failure probabilities of the three cases to be 2.32×10^{-2}, 1.00×10^{-1}, and 6.22×10^{-1} using only 21, 18, and 12 structural analyses, respectively.

Fig. 11 shows how the probabilities from MCS for the three cases converged as the number of samples increased. The probability converged very quickly in Case 3 because the expected probability level (i.e., 6.22×10^{-1}, shown by the blue dotted line) was relatively high. On the other hand, probability convergence was not achieved even with 1000 samples in Case 1 because the expected probability level (i.e., 2.32×10^{-2}, shown by the blue dotted line) was very small. Unlike the proposed method, the level of the accuracy of the estimated failure probability in the MCS-based method depends significantly on the number of samples (i.e. simulations).

Table 3 Three selected cases

Case name	Input ground motion	PGA (g)	Limit State	Failure probability with propose method	Number of structural analyses
Case 1	Set02-01	0.08	Serviceability	2.32×10^{-2}	21
Case 2	Set03-04	0.35	Damage control	1.00×10^{-1}	18
Case 3	Set01-05	0.25	Collapse prevention	6.22×10^{-1}	12

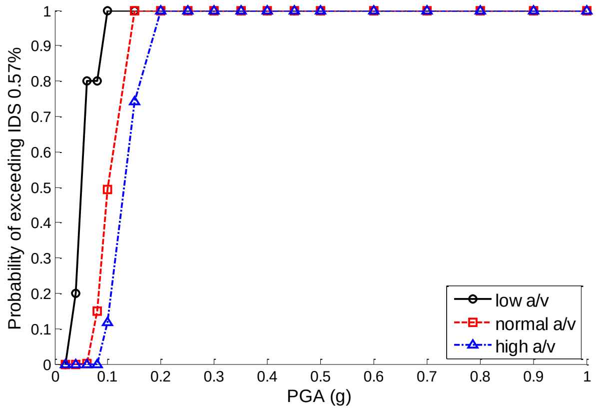

(a) Serviceability limit state

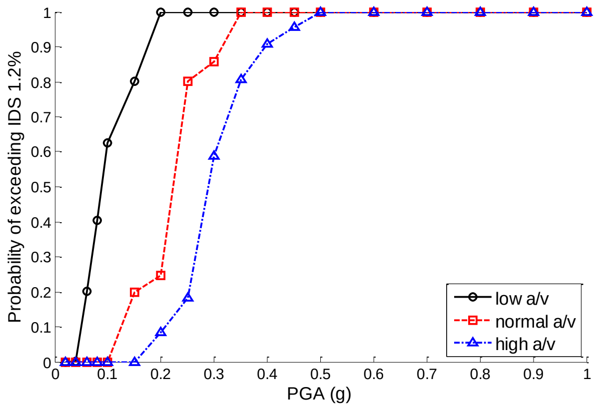

(b) Damage control limit state

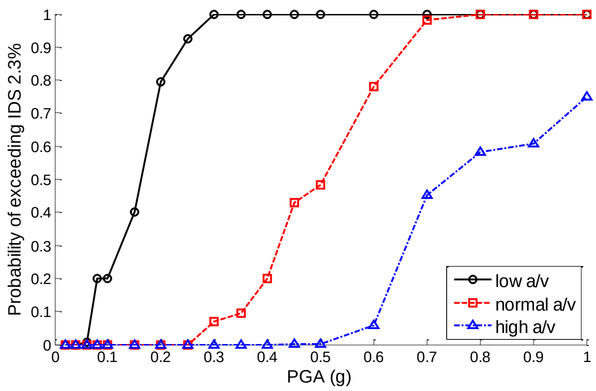

(c) Collapse prevention limit state

Fig. 10 Fragility curves from component reliability analysis for three limit states

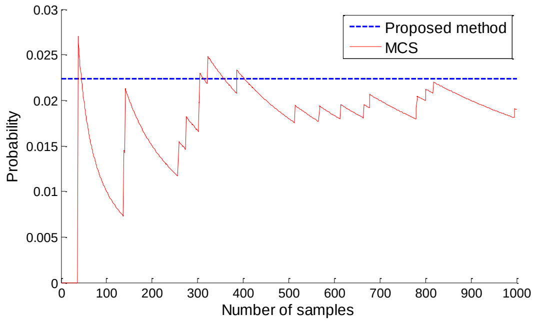

(a) Case 1

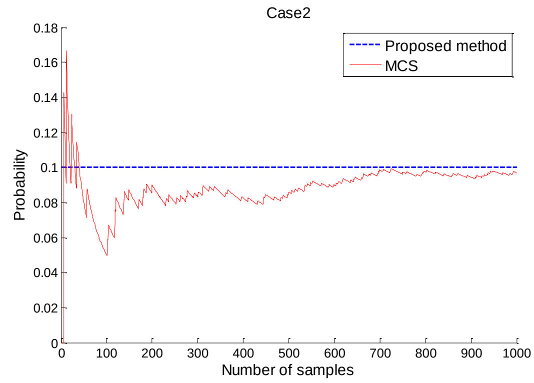

(b) Case 2

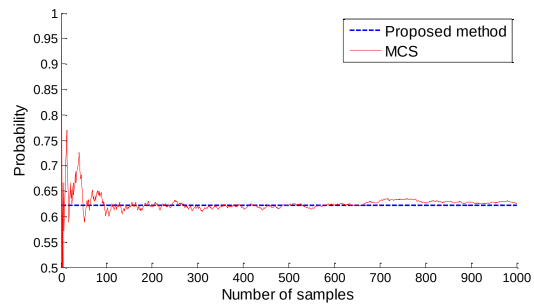

(c) Case 3

Fig. 11 Probabilities from MCS with increasing number of samples for the three cases

Overall, the proposed FORM-based method required a small number of limit-state function evaluations (or structural analyses). The required number of limit-state function evaluations n_{fe} can be calculated by using Eq. (7). In the selected numerical example, the maximum cost of the structural analyses by the proposed method was 60 because there were two random variables and a maximum of 20 iterations. The computational cost can be reduced further when convergence is achieved early during FORM, as shown in Table 3.

In some cases, the computational efficiency of the proposed method may suffer, especially when there are many random variables in a problem. As shown in Eq. (7), the required number of limit-state function evaluations n_{fe} is proportional to (n_{RV} + 1). Thus, depending on the number of random variables, using one of the advanced simulation-based methods may be more preferable. In many cases, however, several random variables are enough to represent the uncertainties in the structure, and the proposed method can be useful for such cases.

In the proposed method, convergence may not be achieved during FORM depending on the shape of the limit-state surface. If the failure domain of interest is very complex the proposed method may not work properly. In such a case, another method introducing more advanced simulation-based/non-simulation-based techniques may be needed.

4.2.2 Seismic fragility curves from system reliability analysis

As discussed in Sec. 3.2, FORM enables system reliability analysis through the use of component reliability analysis results (i.e., the probabilities of component events and their correlations). In Eqs. 11(a)–(c), the three limit states are expressed by "component" events where the maximum inter-story drift ratio among the twelve columns exceeds certain thresholds. However, they can also be described by "system" events as follows

$$\text{Serviceability:} \quad P_{1,sys} = P\left[\bigcup_{i=\mathrm{C01},\ldots,\mathrm{C24}} g_{1,i}(\mathbf{x}) \le 0\right] = P\left[\bigcup_{i=\mathrm{C01},\ldots,\mathrm{C24}} \left(0.0057 - ISD_i(\mathbf{x})\right) \le 0\right] \quad \text{(12a)}$$

$$\text{Damage control:} \quad P_{2,sys} = P\left[\bigcup_{i=\mathrm{C01},\ldots,\mathrm{C24}} g_{2,i}(\mathbf{x}) \le 0\right] = P\left[\bigcup_{i=\mathrm{C01},\ldots,\mathrm{C24}} \left(0.012 - ISD_i(\mathbf{x})\right) \le 0\right] \quad \text{(12b)}$$

$$\text{Collapse prevention:} \quad P_{3,sys} = P\left[\bigcup_{i=\mathrm{C01},\ldots,\mathrm{C24}} g_{3,i}(\mathbf{x}) \le 0\right] = P\left[\bigcup_{i=\mathrm{C01},\ldots,\mathrm{C24}} \left(0.023 - ISD_i(\mathbf{x})\right) \le 0\right] \quad \text{(12c)}$$

where $ISD_i(\cdot)$ denotes the inter-story drift ratios of the twelve columns. In the equations, each limit state is defined by a series system event consisting of twelve component events representing the failure of the twelve columns based on the limit state. In many structural reliability problems, such system event description is effective and can provide better accuracy in probability calculations, especially for large or highly complex structures.

Fig. 12 shows the fragility curves from the system reliability analysis using Eqs. (12(a)-12(c)). Compared with the curves from the component reliability analysis in Fig. 10, these curves show very little difference that may not be seen in the figures clearly. This is because the target structure of this numerical example is assumed to be a low-rise structure which is a relatively small and simple structure. To investigate this issue further, we considered Cases 1–3 in Table 3: when performing component reliability analysis using Eqs. (11(a)-11(c)), the failure probabilities for Cases 1, 2, and 3 were estimated to be 2.32×10^{-2}, 1.00×10^{-1}, and 6.22×10^{-1}, respectively.

In order to compute the system failure probabilities from Eqs. (12(a)-12(c)), component reliability analysis must be performed for each of the twelve columns. The component failure probabilities for the three cases are shown in Table 4. Each case had several dominant component events (e.g., C11–C14 for Case 3) and zero-probability events (e.g., C01–C04 and C21–C24 for Case 3). Case 2 had only one non-zero component probability with C11. For the system reliability analysis, the component events with zero probability were ignored. The correlation coefficient matrix was then constructed using $\rho_{ij} = -\boldsymbol{\alpha}_i\boldsymbol{\alpha}_j^{\mathrm{T}}$, as shown in Table 5. A correlation coefficient matrix was not constructed for Case 2 because there was only one non-zero component event. The table shows that the correlation values between dominant component events were very high. Based on the component failure probabilities and correlation matrix, the system failure probabilities for the three cases were calculated to be 2.46×10^{-2}, 1.00×10^{-1}, and 6.23×10^{-1}, respectively. Compared with the results from component reliability analysis (shown in Table 3), it is observed that the differences are very small. Because the target structure is relatively small and simple, the twelve columns assumed to share the same random variables representing their concrete and steel strengths and there was the high correlation between the dominant component events. This made the system probability very close to the maximum of the component probabilities.

Table 4 Component failure probabilities for Cases 1–3

Case name	Failure Probability ($\times 10^{-1}$)											
	C01	C02	C03	C04	C11	C12	C13	C14	C21	C22	C23	C24
Case 1	0	0	0	0	0	0.24	0.25	0.22	0	0	0	0
Case 2	0	0	0	0	1.00	0	0	0	0	0	0	0
Case 3	0	0	0	0	6.16	6.18	6.12	6.13	0	0	0	0

Table 5 Correlation coefficient matrices for Cases 1 and 3

Correlation (Case 1)	C12	C13	C14
C12	1	0.9999	0.9995
C13		1	0.9991
C14	Symmetric		1

Correlation (Case 3)	C11	C12	C13	C14
C11	1	0.9995	0.9999	0.9996
C12		1	0.9992	0.9999
C13			1	0.9992
C14	Symmetric			1

Although system reliability turned out to be unnecessary in this numerical example, it may make a significant difference to structural fragility when a structure is relatively large so that spatial variability of material properties needs to be assumed. In such cases, fragility curves should be developed at the system level with the proposed method, but the computational cost will increase. As the selected numerical example, system reliability analysis may not be essential especially for low-rise structures which would be constructed in a relatively short time because there would be no significant variability of material properties.

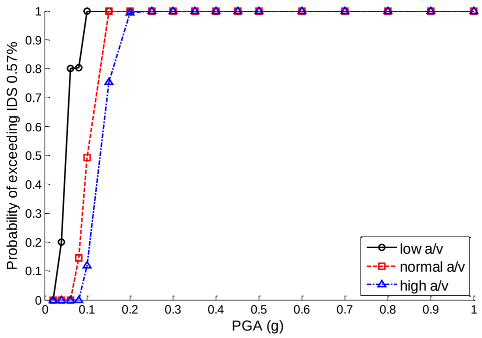

(a) Serviceability limit state

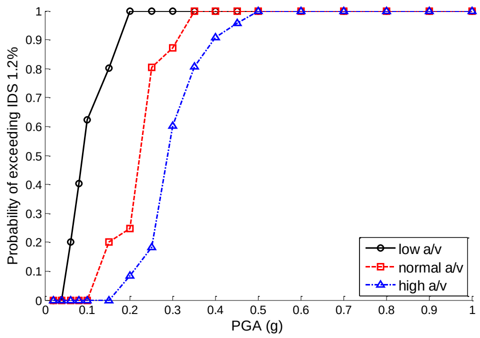

(b) Damage control limit state

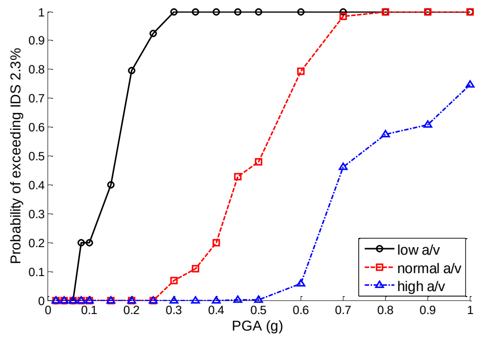

(c) Collapse prevention limit state

Fig. 12 Fragility curves from system reliability analysis for three limit states

5. Conclusions

This paper introduces a new method for the development of seismic fragility curves. The new method proposes the integration of sophisticated software packages for reliability and structural analyses to generate more accurate seismic fragility curves for less computational cost than simulation-based methods. FERUM-ZEUS was developed as a computational platform for the proposed method: on this platform, the reliability analysis package FERUM repeatedly calls ZEUS-NL to obtain structural responses of interest during component reliability analysis. Because the proposed method performs reliability analysis using the first-order reliability method, it provides component probabilities as well as useful byproducts and allows the development of fragility curves of a structure at the system level. The new method was applied to the numerical example of a 2D frame structure. The results were compared with those from Monte Carlo simulation, and the proposed method was found to generate seismic fragility curves more accurately and efficiently. The effect of system reliability analysis was also investigated to evaluate its necessity. Although system reliability analysis was not strictly necessary for the numerical example explored in this study, it may make a significant difference in structural fragility estimates particularly for large-scale structures or when spatial variability of material properties needs to be considered. The results with the numerical example proved that the proposed method can obtain accurate seismic fragility curves at a moderate computational cost.

Acknowledgements

This research was supported by a grant(14SCIP-B065985-02) from Smart Civil Infrastructure Research Program funded by Ministry of Land, Infrastructure and Transport(MOLIT) of Korea government and Korea Agency for Infrastructure Technology Advancement(KAIA). The authors would like to thank Dr. Oh-Sung Kwon (University of Toronto) for his structural model and valuable comments.

References

Ambartzumian, R., Der Kiureghian, A., Ohanian V. and Sukiasian, H. (1998), “Multinormal probability by sequential conditioned importance sampling: theory and application”, *Probabilist. Eng. Mech.*, **13**(4), 299-308.

Bracci, J.M., Reinhorn, A.M. and Mander, J.B. (1992), *Seismic Resistance of Reinforced Concrete Frame Structures Designed Only for Gravity Loads: Part I—Design and Properties of a One-third Scale Model Structure*, Technical report, National Center for Earthquake Engineering Research, Buffalo, NY, USA.

Calvi, G.M., Pinho, R., Magenes, G., Bommer, J.J., Restrepo-Velez, L.F. and Crowley, H. (2006), “Development of seismic vulnerability assessment methodologies over the past 30 years”, *ISET J. Earthqu. Technol.*, **43**(3), 75-104.

DesRoches, R., Comerio, M., Eberhard, M., Mooney, W. and Rix, G.J. (2011), “Overview of the 2010 Haiti Earthquake”, *Earthq. Spectra*, **27**(1), 1-21.

Der Kiureghian, A. (2005), *First- and second-order reliability methods*, Engineering Design Reliability Handbook, (Eds., Nikolaidis, E., Ghiocel, D.M. and Singhal, S.), CRC Press, Boca Raton, FL, USA, Chap. 14.

Der Kiureghian, A. and Taylor, R.L. (1983), "Numerical methods in structural reliability", *Proceedings of the 4th International Conference on Applications of Statistics and Probability in Civil Engineering (ICASP4)*, Florence, Italy, June.

Ditlevsen, O. (1979), "Narrow reliability bounds for structural systems", *J. Struct Mech*, **7**(4), 453-472.

Elnashai, A., Hampton, S., Karaman, H., Lee, J.S., McLaren, T., Myers, J., Navarro, C., Sahin, M., Spencer, B. and Tolbert, N. (2008), "Overview and applications of MAEviz – HAZTURK 2007", *J. Earthq. Eng.*, **12**(1), 100-108.

Elnashai, A.S., Papanikolaou, V.K. and Lee, D. (2010), *ZEUS NL - A System for Inelastic Analysis of Structures*, User's manual, Mid-America Earthquake (MAE) Center, Department of Civil and Environmental Engineering, University of Illinois at Urbana-Champaign, Urbana, IL, USA.

Genz, A. (1992), "Numerical computation of multivariate normal probabilities", *J. Comput. Graph. Stat.*, 141-149.

Gollwitzer, S., Kirchgaßner, B., Fischer, R. and Rackwitz, R. (2006), "PERMAS-RA/STRUREL system of programs for probabilistic reliability analysis", *Struct. Saf.*, **28**(1-2), 108-129.

Haldar, A. (2006), *Recent developments in reliability-based civil engineering*, World Scientific Publishing Company, Singapore.

Haldar, A. and Mahadevan, S. (2000), *Probability, Reliability, and Statistical Methods in Engineering Design*, John Wiley & Sons, New York, NY, USA.

Haukaas, T. (2003), "Finite element reliability and sensitivity methods for performance-based engineering", Ph.D. Dissertation, University of California, Berkeley, CA, USA.

Hohenbichler, H. and Rackwitz, R. (1983), "First-order concepts in system reliability", *Struct. Saf.*, **1**(3), 177-188.

Jeong, S. and Elnashai, A.S. (2007), "Probabilistic fragility analysis parameterized by fundamental response quantities", *Eng. Struct.*, **29**, 1238-1251.

Kang, W.H. (2011), *Development and application of new system reliability analysis methods for complex infrastructure systems*, Ph.D. Dissertation, University of Illinois, Urbana-Champaign, IL, USA.

Kang, W.H. and Song, J. (2010), "Evaluation of multivariate normal integrals for general systems by sequential compounding", *Struct. Saf.*, **32**(1), 35-41.

Kang, W.H., Lee, Y.J., Song, J. and Gencturk, B. (2012), "Further development of matrix-based system reliability method and applications to structural systems", *Struct. Infrastruct. E.*, **8**(5), 441-457.

Kircher, C.A., Whitman, R.V. and Holmes, W.T. (2006), "HAZUS earthquake loss estimation methods", *Nat. Hazards*, **7**(2), 45-59.

Kwon, O.S. (2007), *Probabilistic seismic assessment of structure, foundation, and soil interacting systems*, Ph.D. Dissertation, University of Illinois, Urbana, IL, USA,

Kwon, O.S. and Elnashai, A.S. (2006), "The effect of material and ground motion uncertainty on the seismic vulnerability curves of RC structure", *Eng. Struct.*, **28**(2), 289-303.

Lee, Y.J. and Song, J. (2011), "Risk analysis of fatigue-induced sequential failures by branch-and-bound method employing system reliability bounds", *J. Eng. Mech. - ASCE*, **137**(12), 807-821.

Lee, Y.J. and Song, J. (2012), "Finite-element-based system reliability analysis of fatigue-induced sequential failures", *Reliab. Eng. Syst. Safe.*, **108**, 131-141.

Lee, Y.J., Song, J. and Tuegel, E.J. (2008), "Finite element system reliability analysis of a wing torque box", *Proceedings of the 10th AIAA Nondeterministic Approaches Conference*, Schaumburg, IL, April.

Liu, P.L., Lin, H.Z. and Der Kiureghian, A. (1989), *CalREL User Manual*. Report No. UCB/SEMM-89/18, University of California, Berkeley, CA, USA.

Melchers, R.E. (1999), *Structural Reliability: Analysis and Prediction*, (2nd Ed.), John Wiley & Sons, New York, NY, USA.

NIBS (1999), *HAZUS, Earthquake Loss Estimation Technology*, Technical Manual prepared by the National Institute of Buildings Sciences (NIBS) for the Federal Emergency Management Agency (FEMA).

Pandey, M.D. (1998), "An effective approximation to evaluate multinormal integrals", *Struct. Saf.*, **20**, 51-67.

Rackwitz, R. and Fiessler, B. (1978), "Structural reliability under combined load sequences", *Comput. Struct.*, **9**, 489-494.

Rossetto, T. and Elnashai, A.S. (2003), "Derivation of vulnerability functions for European-type RC structures based on observational data", *Eng. Struct.*, **25**(10), 1241-1263.

Song, J. (2007), *Decision and Risk Analysis*, Lecture notes, University of Illinois, Urbana, IL, USA, Feb. 28.

Song, J. and Der Kiureghian, A. (2003), "Bounds on system reliability by linear programming", *J. Eng. Mech. - ASCE*, **129**(6), 627-636.

Song, J. and Kang, W.H. (2009), "System reliability and sensitivity under statistical dependence by matrix-based system reliability method", *Struct. Saf.*, **31**(2), 148-156.

SwRI. (2011), *NESSUS (ver 9.6)*, Southwest Research Institute, http://www.nessus.swri.org/ [cited 1 Mar. 2013].

CY